Hypersensitivity to perturbation in the quantum kicked top

Rüdiger Schack,[1] Giacomo M. D'Ariano,[2] and Carlton M. Caves[1]
[1] *Center for Advanced Studies, Department of Physics and Astronomy, University of New Mexico, Albuquerque, New Mexico 87131-1156*
[2] *Dipartimento di Fisica "Alessandro Volta," Università degli Studi di Pavia, Via A. Bassi 6, 27100 Pavia, Italy*
(Received 28 March 1994)

For the quantum kicked top we study numerically the distribution of Hilbert-space vectors evolving in the presence of a small random perturbation. For an initial coherent state centered in a chaotic region of the classical dynamics, the evolved perturbed vectors are distributed essentially like random vectors in Hilbert space. In contrast, for an initial coherent state centered near an elliptic (regular) fixed point of the classical dynamics, the evolved perturbed vectors remain close together, explore only a few dimensions of Hilbert space, and do not explore them randomly. These results support and extend the results of earlier studies, thereby providing additional support for a characterization of quantum chaos that uses concepts from information theory.

PACS number(s): 05.45.+b, 89.70.+c, 03.65.−w

I. INTRODUCTION

In a series of previous papers [1–4], two of the authors introduced a characterization of Hamiltonian chaos which is directly applicable to quantum as well as to classical systems. This characterization, formulated in the framework of statistical mechanics, is based on the following question: How much information is needed to predict an evolved system state in the presence of random perturbations? General arguments [2] and an investigation of the symbolic dynamics of the baker's map [4] provide strong evidence that chaotic classical Hamiltonian systems show what we call *hypersensitivity to perturbation*, i.e., a rapid increase with the number of time steps of the information needed to describe the perturbed time evolution of a system state, the information attaining values exponentially larger than the increase of ordinary entropy that results from averaging over the perturbation.

Hypersensitivity to perturbation explains quantitatively how information about the state of a system is lost through interaction with an incompletely known environment and therefore is important for understanding why entropy necessarily increases in systems that are not perfectly isolated. The connection of this work on chaos with statistical physics is developed in Sec. VI. In addition to its straightforward motivation in statistical mechanics, the concept of hypersensitivity to perturbation may provide a more physical way to characterize quantum chaos [2]. Numerical simulations [1] show that the quantum baker's map [5] displays hypersensitivity to perturbation.

In this paper, we analyze how hypersensitivity to perturbation arises in the quantum kicked top [6,7], a system whose classical dynamics has both chaotic and regular regions. To shed light on the reason for the rapid increase of information associated with the property of hypersensitivity to perturbation, we perform a detailed numerical analysis of how the vectors arising from different perturbation histories (realizations of the random perturbation) are distributed in Hilbert space. For an initial coherent state centered in a chaotic region of the classical dynamics, the evolved perturbed vectors are distributed essentially like random vectors in Hilbert space. In contrast, for an initial coherent state centered near an elliptic (regular) fixed point of the classical dynamics, the evolved perturbed vectors remain close together, explore only few dimensions of Hilbert space, and do not explore those dimensions randomly.

Quantum systems show no "sensitivity to initial conditions," due to unitarity, but they show what one might call sensitivity to parameters in the Hamiltonian, as has been demonstrated for the kicked top by Peres [8]. Peres compares the time evolution of the same initial Hilbert-space vector for two slightly different values of the twist parameter in the kicked-top Hamiltonian (see Sec. II). He finds that, after a fixed number of time steps, the two evolved vectors are far apart if the initial vector is a coherent state centered in a chaotic region of the classical dynamics, but the two evolved vectors stay close together if the initial coherent state is centered near an elliptic fixed point of the classical dynamics.

Our approach to quantum chaos could be viewed as a generalization of Peres's work: while Peres studies time evolution due to an incompletely known Hamiltonian, we analyze the distribution of vectors arising from time evolution under a stochastic Hamiltonian. There is, however, a fundamental difference in philosophy between the two approaches, which can be understood fully only in the context of statistical mechanics. This difference becomes apparent in Sec. VI.

The quantum kicked top, its classical limit, and the concept of a coherent state are reviewed in Sec. II. Section III defines the perturbations used in the numerical simulations. In Sec. IV we explain how the distribution of vectors in Hilbert space is connected to questions of information and entropy and how the numerical data are compiled into figures. Section V contains the numerical results of this paper. Finally, in Sec. VI, we discuss the

implications of our results for the foundations of statistical physics.

II. THE KICKED TOP

The quantum model of the kicked top [6,7] describes a spin-J particle—i.e., an angular momentum vector $\hbar\hat{\mathbf{J}} = \hbar(\hat{J}_x, \hat{J}_y, \hat{J}_z)$, where $[\hat{J}_i, \hat{J}_j] = i\epsilon_{ijk}\hat{J}_k$—whose dynamics in $(2J+1)$-dimensional Hilbert space is governed by the Hamiltonian

$$\hat{H}(t) = (\hbar p/T)\hat{J}_z + (\hbar k/2J)\hat{J}_x^2 \sum_{n=-\infty}^{+\infty} \delta(t - nT) . \quad (2.1)$$

The free precession of the spin around the z axis (first term in the Hamiltonian) is interrupted periodically by sudden kicks or *twists* at times nT with twist parameter k (second term in the Hamiltonian). The angle of free precession between kicks is given by p. In this paper we always use $p = \pi/2$.

We look at the time evolution of an initial Hilbert-space vector $|\psi_0\rangle$ at discrete times nT. After n time steps, the evolved vector is given by

$$|\psi_n\rangle = \hat{U}_k^n |\psi_0\rangle , \quad (2.2)$$

where $\hat{U}_k$ is the unitary Floquet operator:

$$\hat{U}_k = \exp[-i(k/2J)\hat{J}_x^2] \exp(-i\pi\hat{J}_z/2) . \quad (2.3)$$

The classical Poincaré map corresponding to the quantum map is obtained by introducing the unit vector $\vec{\omega} = (X, Y, Z) \equiv \hat{\mathbf{J}}/J$ and performing the limit $J \to \infty$. One obtains [7]

$$\begin{aligned} X' &= -Y , \\ Y' &= X\cos kY + Z\sin kY , \\ Z' &= Z\cos kY - X\sin kY . \end{aligned} \quad (2.4)$$

The map (2.4) is an area-preserving map of the unit sphere, i.e., an area-preserving map on the configuration space of a classical spin with fixed magnitude. Depending on the value of the twist parameter k, this map has regions of chaotic behavior interspersed with regular regions associated with elliptic cyclic points. In this paper, we are interested in two cyclic points of the map for $k = 3$. One is an elliptic fixed point of period 1 located at [9]

$$Z = \cos\theta = 0.455\,719 , \quad \varphi = 3\pi/4 , \quad (2.5)$$

where we have used spherical coordinates

$$\theta = \arccos Z , \quad \varphi = \arctan Y/X . \quad (2.6)$$

The elliptic fixed point (2.5) is surrounded by an oval-shaped regular region, extending about 0.3 rad in the φ direction and about 0.5 rad in the θ direction. The other cyclic point of interest to us is a hyperbolic fixed point of period 4, which has a positive Lyapunov exponent. It is located in the middle of a chaotic region at [9]

$$Z = \cos\theta = 0.615\,950 , \quad \varphi = \pi/4 . \quad (2.7)$$

We choose the two fixed points (2.5) and (2.7) instead of the extreme elliptic ($\varphi = n\pi/4$, $Z = 0$) and hyperbolic ($Z = \pm 1$) points described in Ref. [9], because the latter suffer accidental invariance with respect to one or both of the perturbation operators considered in Sec. III.

The model has a conserved parity, which for half-integer J takes the form

$$\hat{S} = -i\exp(-i\pi\hat{J}_z) \quad (2.8)$$

and which permits factorization of the matrix representation of the operator $\hat{U}$ into two blocks. Starting from a state with definite parity, the whole dynamical evolution occurs in the invariant Hilbert subspace with the given parity. For half-integer J, the dimension of the even-parity subspace (eigenspace of $\hat{S}$ with eigenvalue 1) is $J + \frac{1}{2}$. In this paper, we work with $J = 511.5$ in the 512-dimensional even-parity subspace. We consider only the projection of the initial vector in the even subspace. Numerical evidence and symmetry considerations [8] suggest that no additional insight is gained by including the odd-parity subspace. In any case, the restricted model can be regarded as a quantum map in its own right, which can be investigated independently of the behavior of the complete kicked-top model.

We want to choose initial vectors for the quantum evolution that correspond as closely as possible to the classical directions (2.5) and (2.7). For this purpose, coherent states [10–12] are appropriate. The coherent state $|\theta, \varphi\rangle$ is defined by the relation

$$\mathbf{n}\cdot\hat{\mathbf{J}}|\theta,\varphi\rangle = J|\theta,\varphi\rangle , \quad (2.9)$$

where $\mathbf{n}$ is the unit vector pointing in the direction given by θ and φ. All coherent states can be generated by an appropriate rotation of the state $|J, M = J\rangle = |\theta = \pi/2, \varphi = 0\rangle$, where $|J, M\rangle$ $(M = -J, \ldots, J)$ is the common eigenstate of $\hat{J}^2$ and $\hat{J}_z$ with eigenvalues $J(J+1)$ and M, respectively. In calculations, it is convenient to use the explicit representation

$$|\theta,\varphi\rangle = \sum_{n=0}^{2J} \sqrt{P_J(\theta,n)}\, e^{in\varphi} |J, n - J\rangle , \quad (2.10)$$

where

$$P_J(\theta,n) = \binom{2J}{n} \left(\frac{1+\arccos\theta}{2}\right)^{2J-n} \left(\frac{1-\arccos\theta}{2}\right)^{n} . \quad (2.11)$$

In the following we need a metric on Hilbert space. The distance between two normalized vectors $|\psi_1\rangle$ and $|\psi_2\rangle$ is defined as the Hilbert-space angle

$$s(|\psi_1\rangle, |\psi_2\rangle) = \cos^{-1}(|\langle\psi_1|\psi_2\rangle|) \equiv \phi \quad (2.12)$$

between the two vectors [13]. Consider two coherent states $|\theta,\varphi\rangle$ and $|\theta',\varphi'\rangle$. In terms of the angle α between the directions (θ,φ) and (θ',φ'), the distance between the two coherent states is given by [14]

$$\cos[s(|\theta,\varphi\rangle,|\theta',\varphi'\rangle)] = |\langle\theta,\varphi \mid \theta',\varphi'\rangle| = [\cos(\alpha/2)]^{2J} \simeq \exp(-J\alpha^2/4) , \tag{2.13}$$

where the approximation is valid for large J. Two coherent states can therefore be regarded as roughly orthogonal if $\alpha \gtrsim 2J^{-1/2}$ [8]. The *size* of the coherent state $|\theta,\varphi\rangle$ is conveniently defined in terms of the Q function

$$Q_{\theta,\varphi}(\theta',\varphi') \equiv |\langle\theta',\varphi' \mid \theta,\varphi\rangle|^2 = [\cos(\alpha/2)]^{4J} \equiv Q(\alpha) . \tag{2.14}$$

Since $Q(2J^{-1/2}) \simeq e^{-2}Q(0)$, the Q function of the coherent state $|\theta,\varphi\rangle$ is very small outside a region of radius $2J^{-1/2}$ centered at the direction (θ,φ). For the value $J = 511.5$ used in this paper, one finds a radius of $2J^{-1/2} \simeq 0.09$ rad, less than the size of the regular region around the elliptic fixed point (2.5).

III. PERTURBED EVOLUTION

Our goal is to quantify how much information is required to track the state of a system when, instead of being wholly isolated, it is perturbed by interaction with its environment. In classical physics, interactions with an incompletely known environment can be described by a stochastic Hamiltonian, each realization of which corresponds to a particular initial condition for the environment. The situation is more complicated in quantum mechanics. Due to the possible entanglement of system and environment, there is no way to associate a unique perturbation history with a given initial condition of the environment. An upcoming work discusses how to study hypersensitivity to perturbation in a realistic model of a quantum system interacting with an environment. For the present paper we restrict ourselves to the special case of quantum time evolution under a stochastic Hamiltonian.

The problem is simplified further by considering only two possible unitary time evolutions at each step. These two time evolution operators we denote by $\hat{U}^+$ and $\hat{U}^-$. A perturbed time step consists in applying either $\hat{U}^+$ or $\hat{U}^-$ with equal probability. After n time steps, the number of different perturbation sequences is 2^n, each sequence having probability 2^{-n}.

We use two different perturbations: (i) the *twist perturbation*, defined by choosing the twist parameter k at random from step to step, the two possible Floquet operators being given by [8]

$$\hat{U}^+ = \hat{U}_k , \quad \hat{U}^- = \hat{U}_{k+\epsilon} ; \tag{3.1}$$

and (ii) the *turn perturbation*, defined by rotating the spin by a small angle ϵ around the z axis after each unperturbed step $\hat{U}_k$, the two possible Floquet operators being given by

$$\hat{U}^+ = \exp(-i\epsilon\hat{J}_z)\,\hat{U}_k , \quad \hat{U}^- = \exp(+i\epsilon\hat{J}_z)\,\hat{U}_k . \tag{3.2}$$

Notice that the time-evolution operators (3.1) and (3.2) commute with parity (2.8) and hence do not couple odd- and even-parity subspaces.

For perturbation strengths we use $\epsilon = 0.03$ and $\epsilon = 0.003$ for the twist perturbation and $\epsilon = 0.003$ for the turn perturbation. For a twist parameter $k + \epsilon$ the zenithal location of the fixed points (2.5) and (2.7) changes slightly to $Z = 0.443\,579$ and $Z = 0.619\,848$ for $\epsilon = 0.03$ and to $Z = 0.454\,497$ and $Z = 0.616\,341$ for $\epsilon = 0.003$. This corresponds to changes in the zenithal angle θ of $\Delta\theta \simeq 0.014$ rad and $\Delta\theta \simeq 0.005$ rad for $\epsilon = 0.03$ and to $\Delta\theta \simeq 0.0014$ rad and $\Delta\theta \simeq 0.0005$ rad for $\epsilon = 0.003$. All these angles, as well as the angle $\epsilon = 0.003$ we use for the turn perturbation, are very small compared to the size of the elliptic region around the fixed point (2.5) and are also much smaller than the size of a coherent state.

IV. DISTRIBUTION OF VECTORS AND INFORMATION

The 2^n different perturbation sequences obtained by applying every possible sequence of $\hat{U}^-$ and $\hat{U}^+$ for n time steps lead to a list of 2^n vectors, each having probability 2^{-n}. In this section, we explain how the distribution of these 2^n vectors in Hilbert space is related to information and entropy.

Let us start with a slightly more general situation. Imagine we are given a list of N vectors in D-dimensional Hilbert space, $|\psi_1\rangle,\ldots,|\psi_N\rangle$, with probabilities $p_1,\ldots,p_N$. Together with our knowledge of the system Hamiltonian and boundary conditions, the list of vectors with their probabilities constitutes our *background information*. We ask for the average information needed to specify a single one of these vectors, given the background information. The information to specify a particular vector can be quantified either via conditional algorithmic information [15] or by the length of a code word in some coding scheme [16]. In both cases, it is a consequence of the variable-length coding theorem [16] that the information averaged over all vectors, or *average information*, is bounded below by

$$\Delta I = -\sum_{i=1}^{N} p_i \log_2 p_i . \tag{4.1}$$

(Throughout this paper, information and entropy are measured in bits.) There exist coding schemes—an example is Huffman coding [17]—where $\Delta I + 1$ is an upper bound for the average information or code word length. It can be shown [18] that there exists a universal computer for which $\Delta I + 1$ is an upper bound for the average algorithmic information as well. Therefore, we call ΔI the average information, in the sense that the actual average information is within one bit of ΔI if an efficient coding scheme is used. In the case of 2^n equiprobable vectors the average information is $\Delta I = n$.

Suppose some of the N vectors $|\psi_i\rangle$ are very close together in Hilbert space, so that they form a small group. If one is interested in lowering the amount of information ΔI, one may choose to provide just enough information to specify that the actual vector is located in that group, the price being that the entropy of the group is generally

larger than zero. To be more specific, we introduce a coarse graining on Hilbert space defined by a resolution angle ϕ. Vectors less than an angle ϕ apart are grouped together. More precisely, groups are formed in the following way. Starting with the first vector in the list, $|\psi_1\rangle$, the first group is formed of $|\psi_1\rangle$ and of all vectors in the list that are within an angle ϕ of $|\psi_1\rangle$. The same procedure is then repeated with the remaining vectors to form the second group, then the third group, continuing until no ungrouped vectors are left. This grouping of vectors corresponds to a partial averaging over the perturbations. To describe a vector at resolution level ϕ amounts to averaging over those details of the perturbation that do not change the final vector by more than an angle ϕ.

For a given resolution ϕ, there are $N(\phi)$ groups. We denote by N_j the number of vectors in the jth group ($\sum_{j=1}^{N(\phi)} N_j = N$). The N_j vectors in the jth group and their probabilities are denoted by $|\psi_1^j\rangle, \ldots, |\psi_{N_j}^j\rangle$ and $p_1^j, \ldots, p_{N_j}^j$, respectively. Knowing that the system state is in the jth group, but not knowing which state in the jth group is the actual state, corresponds to describing the system by the density operator

$$\hat{\rho}_j = q_j^{-1} \sum_{i=1}^{N_j} p_i^j |\psi_i^j\rangle\langle\psi_i^j| \,, \tag{4.2}$$

where

$$q_j = \sum_{i=1}^{N_j} p_i^j \tag{4.3}$$

is the probability of the jth group given only the background information. For $\phi = \pi/2$, there is only one group, whose density operator, denoted by $\hat{\rho}(\pi/2)$, corresponds to a complete average over the perturbations.

The average information needed to specify which group a vector is in—i.e., the average information needed to specify the system state at resolution level ϕ—is given by

$$\Delta I(\phi) = -\sum_{j=1}^{N(\phi)} q_j \log_2 q_j \,. \tag{4.4}$$

The entropy of the jth group is given by the von Neumann entropy

$$\Delta H^j = -\mathrm{Tr}[\hat{\rho}_j \log_2 \hat{\rho}_j] \,, \tag{4.5}$$

and the average entropy, called *trade-off entropy* in the following, is

$$\Delta H(\phi) = \sum_{j=1}^{N(\phi)} q_j \Delta H^j \,. \tag{4.6}$$

If one chooses to describe the set of vectors not exactly, but only at resolution level ϕ, the average information needed to specify the system state decreases. There is, however, a price: with increasing resolution angle, the uncertainty about the system state increases on the average to a degree quantified by the trade-off entropy.

As a further characterization of the way the vectors are distributed in Hilbert space, we want to define a quantity that indicates how many dimensions of Hilbert space are explored by the vectors in a group. One such quantity would be the dimension of the subspace spanned by the vectors, which is equal to the number of nonzero eigenvalues of $\hat{\rho}_j$. In practice, however, this is not a very useful measure because it cannot discriminate between the case in which all dimensions are occupied with equal weight (all eigenvalues of $\hat{\rho}_j$ roughly equal) and the case in which most vectors are concentrated in a low-dimensional subspace (all eigenvalues of $\hat{\rho}_j$ nonzero, but of strongly varying magnitude).

A possible measure of the number of explored dimensions, which takes into account the small weight of dimensions corresponding to relatively small eigenvalues, is the exponential of the entropy $2^{\Delta H^j}$. This quantity is bounded above by D_j if the vectors are confined to a D_j-dimensional subspace and gets smaller if the dimensions are occupied with different weights. For example, if two eigenvalues of $\hat{\rho}_j$ are close to $\frac{1}{2}$ and all the others are close to zero, then $2^{\Delta H^j} \simeq 2$, indicating that the vectors are essentially confined to a two-dimensional subspace. Unfortunately, for small resolution angles ϕ, ΔH^j is necessarily small just because all the vectors in the group lie along roughly the same direction in Hilbert space; this is true even if the orthogonal components of the vectors are evenly distributed over *all* the orthogonal directions in Hilbert space. For example, the density operator describing a uniform distribution of vectors within a sphere of radius $\phi \ll \pi/2$ has one dominating eigenvalue close to 1 and $D-1$ eigenvalues that are all equal and close to zero (see Appendix B). Clearly, in this case $2^{\Delta H^j}$ is not an adequate measure of the number of dimensions explored. On the other hand, if one could disregard the largest eigenvalue in this example, then the exponential of the entropy would still be a useful measure of the number of explored dimensions.

We therefore introduce the *spread* ΔH_2^j as the entropy calculated with the largest eigenvalue of $\hat{\rho}_j$ omitted. The spread is defined as

$$\Delta H_2^j \equiv -\sum_{k=2}^{D_j} \frac{\lambda_k^j}{1-\lambda_1^j} \log_2\left(\frac{\lambda_k^j}{1-\lambda_1^j}\right) \,, \tag{4.7}$$

where $\lambda_1^j \geq \lambda_2^j \geq \cdots \geq \lambda_{D_j}^j$ are the nonzero eigenvalues of the density operator $\hat{\rho}_j$. The average spread is

$$\Delta H_2(\phi) = \sum_{j=1}^{N(\phi)} q_j \Delta H_2^j \,. \tag{4.8}$$

For a given resolution angle ϕ, the entropy ΔH^j is bounded above by the entropy $H_{D,\max}(\phi)$ of Eq. (B10), which for small ϕ has the value $H_{D,\max}(\phi) \simeq \phi^2 \log_2[e(D-1)/\phi^2]$. The spread ΔH_2^j, on the other hand, can attain its maximum value $\Delta H_2^j = \log_2(D-1)$ for arbitrary resolution angles ϕ. Indeed, the entropy and

the spread are related by

$$\Delta H^j = -\lambda_1^j \log_2 \lambda_1^j - (1-\lambda_1^j)\log_2(1-\lambda_1^j) + (1-\lambda_1^j)\Delta H_2^j \,, \tag{4.9}$$

which indicates how, when there is one dominating eigenvalue, a large spread does not lead to a large entropy.

By giving different weight to dimensions corresponding to different eigenvalues of $\hat{\rho}_j$, the quantity $\lceil 2^{\Delta H_2^j} \rceil$ turns out to be a good indicator of the number of Hilbert-space dimensions explored by the vectors in a group, independent of the size of the region occupied by the group. ($\lceil x \rceil$ denotes the smallest integer greater than or equal to x.) In our analysis of the numerical results, we identify the number of dimensions explored by the total set of N vectors with the integer $n_d \equiv \lceil 2^{\Delta H_2(\pi/2)} \rceil$.

By determining the information $\Delta I(\phi)$, the trade-off entropy $\Delta H(\phi)$, and the average spread $\Delta H_2(\phi)$ as functions of the resolution angle ϕ, a rather detailed picture emerges of how the vectors are distributed in Hilbert space. The information summarizes the distribution of group sizes at the given resolution. The trade-off entropy and the average spread indicate how the vectors are distributed inside the groups.

It is easy to see that information and trade-off entropy obey the inequalities

$$\Delta I(0) \geq \Delta I(\phi) \geq \Delta I(\pi/2) = 0 \tag{4.10}$$

and

$$0 = \Delta H(0) \leq \Delta H(\phi) \leq \Delta H(\pi/2) \,. \tag{4.11}$$

The first inequality in (4.10) follows from the fact that any group at resolution ϕ is the union of groups at resolution $\phi = 0$; in words, the average information needed to specify a group at resolution $\phi = 0$ is equal to the average information needed to specify a group at resolution ϕ *plus* the average information needed to specify $\phi = 0$ groups within the groups at resolution ϕ. The last inequality in Eq. (4.11) is a consequence of the concavity of the von Neumann entropy [19,20]. A general theorem about average density operators [19,20] shows that, for all ϕ,

$$\Delta I(\phi) + \Delta H(\phi) \geq \Delta H(\pi/2) \,. \tag{4.12}$$

In general, $\Delta I(\phi)$ is a decreasing function of ϕ, whereas $\Delta H(\phi)$ is increasing. This monotonicity can sometimes be violated, however, because of discontinuous changes in the grouping of vectors.

As a still further characterization of our list of vectors, we calculate the distribution $g(\phi)$ of Hilbert-space angles $\phi = s(|\psi\rangle, |\psi'\rangle) = \cos^{-1}(|\langle\psi|\psi'\rangle|)$ between all pairs of vectors $|\psi\rangle$ and $|\psi'\rangle$. For vectors distributed randomly in D-dimensional Hilbert space, the distribution function $g(\phi)$ is computed in Appendix A:

$$g(\phi) = \frac{d\mathcal{V}_D(\phi)/d\phi}{\mathcal{V}_D} = 2(D-1)(\sin\phi)^{2D-3}\cos\phi \tag{4.13}$$

[Eq. (A24)]. Here $\mathcal{V}_D(\phi) = (\sin\phi)^{2(D-1)}\mathcal{V}_D$ [Eq. (A18)] is the volume contained within a sphere of radius ϕ in D-dimensional Hilbert space and $\mathcal{V}_D = \pi^{D-1}/(D-1)!$ [Eq. (A22)] is the total volume of Hilbert space. The maximum of $g(\phi)$ is located at $\phi = \arctan(\sqrt{2D-3})$; for large-dimensional Hilbert spaces, $g(\phi)$ is very strongly peaked near the maximum, which is located at $\phi \simeq \pi/2 - 1/\sqrt{2D-3}$, very near $\pi/2$ (see Fig. 1).

V. NUMERICAL RESULTS

In this section we describe the numerical results, which are shown in the figures. In all numerical examples, we use spin $J = 511.5$ and unperturbed twist parameter $k = 3$. The calculations are done in the 512-dimensional even-parity subspace [eigenspace of the parity (2.8) with eigenvalue 1], i.e., effectively in a 512-dimensional Hilbert space. Throughout this section, we use only two different initial states. The first one, the coherent state $|\theta, \varphi\rangle$ with θ and φ given by Eq. (2.5), is centered in a regular region of the classical dynamics; we refer to it as the *regular initial state*. The second one, referred to as the *chaotic*

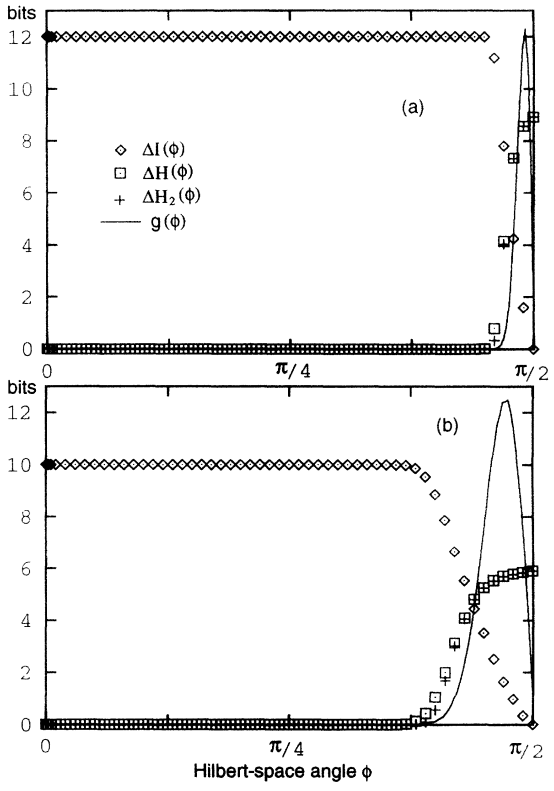

FIG. 1. Distribution of 2^n vectors randomly chosen in D-dimensional Hilbert space. Each diagram shows, as a function of the angle ϕ, the distribution $g(\phi)$ of Hilbert-space angles (unnormalized, in arbitrary units), the average information $\Delta I(\phi)$ to specify a vector at the resolution given by ϕ (in bits), the trade-off entropy $\Delta H(\phi)$ (in bits), and the average spread $\Delta H_2(\phi)$ (in bits). For a precise definition of these quantities, see Sec. IV. (a) $n = 12$, $D = 512$. (b) $n = 10$, $D = 62$.

initial state, is the coherent state $|\theta,\varphi\rangle$ with θ and φ given by Eq. (2.7); the chaotic initial state is centered in a chaotic region of the classical dynamics. Sections V A and V B describe results for the twist perturbation with two different perturbation strengths ϵ. Section V C contains results for the turn perturbation.

A. Twist perturbation: $\epsilon = 0.03$

Applying all possible n-step perturbation sequences, i.e., all possible sequences of n Floquet operators $\hat{U}^-$ and $\hat{U}^+$, to an initial state $|\psi_0\rangle$ generates a set of 2^n equally likely states, as considered in Sec. IV. In Fig. 2 the quantities defined in Sec. IV are computed for the twist perturbation (3.1) with perturbation strength $\epsilon = 0.03$. Figure 2 shows results after 8 and 12 steps for both the chaotic and the regular initial conditions.

In the chaotic case in Fig. 2(a), where the total number of vectors is $2^8 = 256$ (8 steps), the distribution of Hilbert-space angles $g(\phi)$ is concentrated at large angles, i.e., most pairs of vectors are far apart from each other. The small peak of $g(\phi)$ at $\phi \simeq \pi/16$ corresponds to 128 pairs of vectors, the two vectors in each pair being generated by perturbation sequences that differ only at the first step. The somewhat larger peak of $g(\phi)$ at $\phi \simeq 3\pi/16$ similarly indicates the existence of 64 quartets of vectors, generated by perturbation sequences differing only in the first two steps. The information ΔI needed to track a perturbed vector at resolution level ϕ is 8 bits at small angles where each group contains only one vector. At $\phi \simeq \pi/16$ the information drops to 7 bits and at $\phi \simeq 3\pi/16$ it drops to 6 bits, reflecting the grouping of the vectors in pairs and quartets, respectively. For larger resolution angles, the information stays constant before dropping rapidly to zero at angles $\phi \gtrsim 3\pi/8$. Just as the information begins to drop rapidly, there is a sudden drop to about 5 bits, reflecting a further, approximate grouping into 32 octets of vectors, generated by perturbation sequences that differ only in the first three steps. The final drop in the information coincides with the main peak in the angle distribution $g(\phi)$ and with the rising of the trade-off entropy to its maximum value of $\Delta H \simeq 4$ bits. The number of explored dimensions is $n_d = \lceil 2^{\Delta H_2(\pi/2)} \rceil = 19$.

If the number of steps is increased to 12 [see Fig. 2(c)], the main features of Fig. 2(a) are preserved. The discontinuous drops in information—from 12 to 11 and from 11 to 10 bits—due to the formation of pairs and quartets are obvious, but the corresponding peaks in $g(\phi)$ are

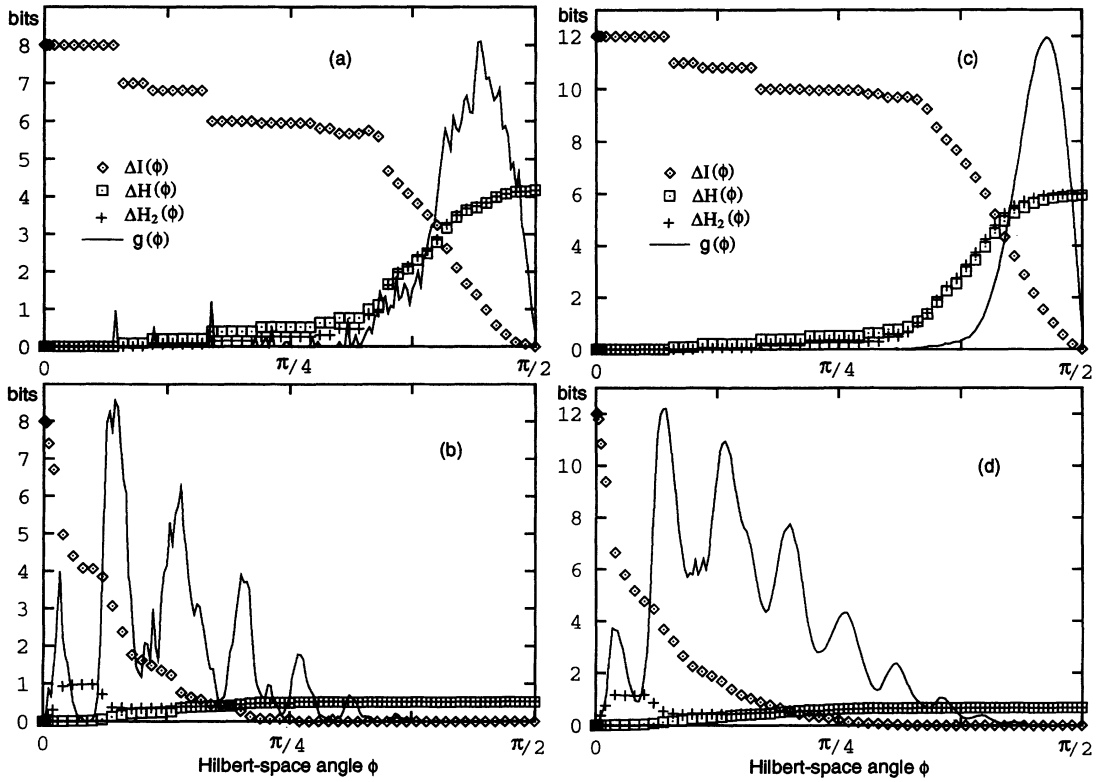

FIG. 2. Results characterizing the distribution of Hilbert-space vectors for the perturbed kicked top with $J = 511.5$ and $k = 3$ in the presence of the twist perturbation (3.1) with $\epsilon = 0.03$. The same quantities as in Fig. 1 are shown. (a) Chaotic case, i.e., initial coherent state $|\theta,\varphi\rangle$ centered in the chaotic region with θ and φ given by Eq. (2.7). Distribution of all 2^8 vectors generated after 8 perturbed steps. (b) Regular case, i.e., initial coherent state centered at the elliptic fixed point given by Eq. (2.5). All 2^8 vectors generated after 8 perturbed steps. (c) Chaotic case. 12 steps, all 2^{12} vectors. (d) Regular case. 12 steps, all 2^{12} vectors.

now almost invisible due to the larger scale produced by the larger total number of pairs of vectors. There is now little evidence of a further grouping into octets. Indeed, Fig. 2(c) suggests that, apart from the organization into pairs and quartets, there is not much structure in the distribution of vectors for a chaotic initial state. The 1024 quartets seem to be rather uniformly distributed in a $n_d = \lceil 2^{\Delta H_2(\pi/2)} \rceil = 65$-dimensional Hilbert space. In order to check that the quartets are indeed more or less randomly distributed in Hilbert space, Fig. 2(c) should be compared to Fig. 1(b), where 1024 random vectors in a 62-dimensional Hilbert space are shown. The random vectors are chosen at random from an ensemble distributed uniformly over Hilbert space [21]. The number of dimensions 62 was chosen by trial and error so that the total entropy $\Delta H(\pi/2)$ came out to be the same in Figs. 2(c) and 1(b). Although the angles between the random vectors are concentrated somewhat more towards larger angles, there is a striking similarity between these two figures.

As further evidence of the nearly random character of the distribution in Fig. 2(c), Fig. 3 compares the eigenvalues of the density operators $\hat{\rho}(\pi/2)$ corresponding to Fig. 2(c) and to the random vectors in Fig. 1(b). The 62 largest eigenvalues in the chaotic case are almost identical to the 62 eigenvalues corresponding to random vectors in 62-dimensional Hilbert space.

The distribution of perturbed vectors starting from the regular initial state is completely different from the chaotic case. Figure 2(b) shows the regular case after eight steps. The angle distribution $g(\phi)$ is conspicuously nonrandom: it is concentrated at angles smaller than roughly $\pi/4$ and there is a regular structure of peaks and valleys. The information drops rapidly, with little plateaus corresponding to the valleys in the angle distribution. The number of explored dimensions is $n_d = 2$, which agrees with results of Peres [8] that show that the quantum evolution in a regular region of the kicked top is essentially confined to a two-dimensional subspace.

Figure 2(d) shows the regular case after 12 steps. The average information and the trade-off entropy show a behavior similar to the 8-step case. The plateaus in the information are washed out, corresponding to less pronounced minima in the distribution of angles. This appearance of formerly forbidden angles is expected as the number of vectors increases; it would occur even for a completely regular array of vectors. The eigenvalues of the density operator $\hat{\rho}(\pi/2)$ corresponding to the 4096 vectors in Fig. 2(d), shown in Fig. 3, confirm the restriction to a two-dimensional subspace. The third-largest eigenvalue, measuring the relative weight of the third explored dimension, is of order only 10^{-2}.

The results shown in Figs. 2 and 3 display a striking difference in the distribution of vectors in the chaotic and regular cases. In the chaotic case, the vectors, aside from the quartet structure, are distributed randomly in a subspace whose dimensionality increases with the number of steps. The information needed to track a perturbed vector after n steps is of the order of n bits, similar to the information needed to specify a vector out of a set of 2^n random vectors. By contrast, in the regular case the vectors do not get far apart in Hilbert space, explore only few dimensions, and do not explore them randomly.

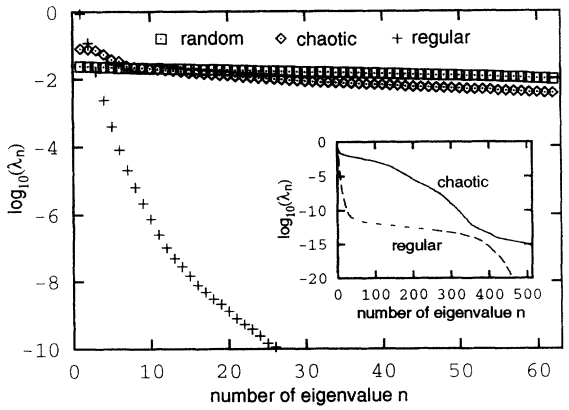

FIG. 3. Eigenvalues of the density operators formed by averaging over random vectors (squares), vectors generated by the perturbed kicked top in the chaotic case (diamonds), and vectors generated by the perturbed kicked top in the regular case (crosses). The density operator in the random case was generated by averaging over 1024 vectors randomly chosen in 62-dimensional Hilbert space. The density operators in the chaotic and regular cases were formed from the 2^{12} vectors in Figs. 2(c) and 2(d), respectively. The main diagram shows, for all three cases, the largest 62 eigenvalues greater than 10^{-10}. The inset shows all eigenvalues greater than 10^{-20} for the chaotic case (solid line) and the regular case (dashed line).

B. Twist perturbation: $\epsilon = 0.003$

Figure 4 shows the distribution of vectors arising from perturbed evolution with a very small twist perturbation of strength $\epsilon = 0.003$. Here, after 12 steps the vectors are not spread very far in Hilbert space. This is true even in the chaotic case, shown in Fig. 4(a), where a typical angle between vectors is $\phi = \pi/8$, the information decreases rapidly with the resolution angle, and only $n_d = 6$ dimensions are explored. Even so, the chaotic case can be easily distinguished from the regular case, shown in Fig. 4(b), where the perturbation has almost no effect on the time evolution of the vectors.

To get a picture of the distribution of vectors for a larger number of steps, Fig. 4(c) shows 4096 vectors selected randomly from the 2^{200} vectors after 200 steps in the chaotic case and Fig. 4(d) shows 1024 vectors selected randomly from the 2^{200} vectors after 200 steps in the regular case. In the chaotic case, the 4096 vectors fill an $n_d = 373$-dimensional subspace quasirandomly, as can be checked by comparison with Fig. 1(a), where results for 4096 random vectors in 512 dimensions are shown. In the regular case, shown in Fig. 4(d), even after 200 steps not more than $n_d = 2$ dimensions are explored. The vectors remain very close together and the information drops rapidly with increasing resolution angle. The difference between the chaotic and regular cases is as striking as in the preceding subsection.

Although the data shown in Fig. 4(c) establish that

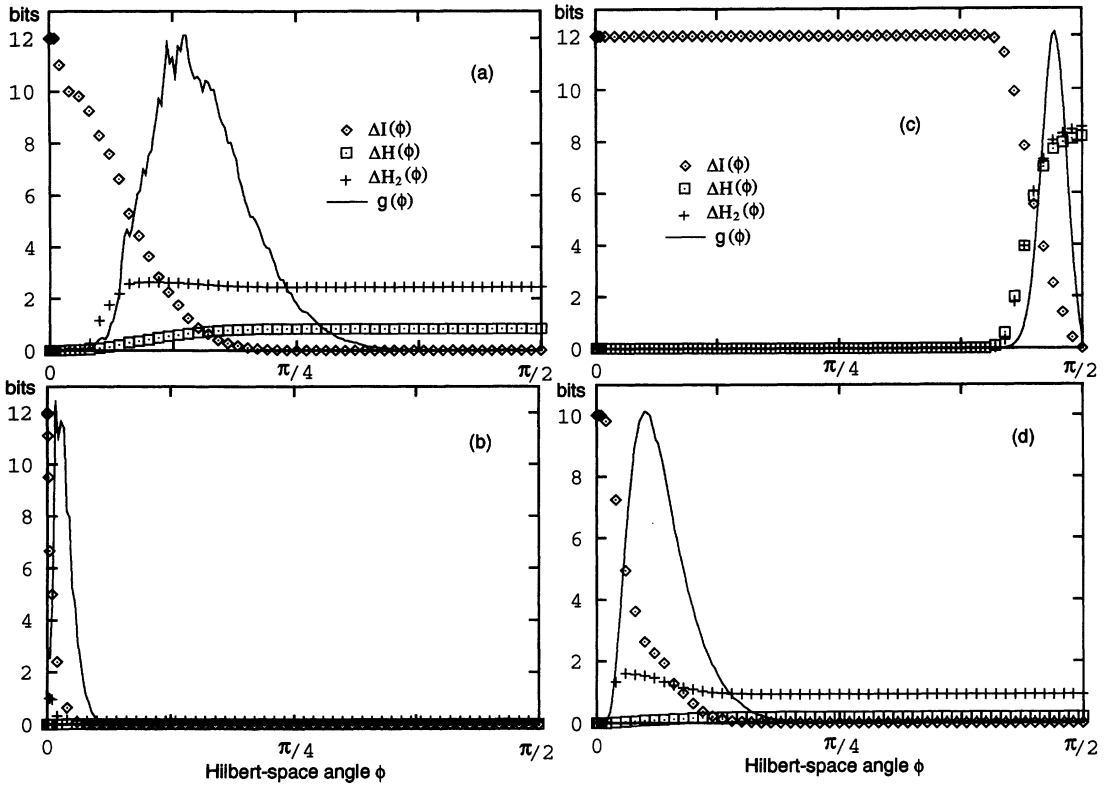

FIG. 4. Same as Fig. 2, but using the twist perturbation (3.1) with $\epsilon = 0.003$. (a) Chaotic case. 12 steps, all 2^{12} vectors. (b) Regular case. 12 steps, all 2^{12} vectors. (c) Chaotic case. 2^{12} vectors randomly chosen after 200 perturbed steps. (d) Regular case. 2^{10} vectors randomly chosen after 200 perturbed steps.

the 4096 vectors selected from the available 2^{200} vectors in the chaotic case fill a large-dimensional space quasi-randomly, they by no means establish that the distribution of all 2^{200} vectors is similar to the distribution of 2^{200} random vectors. For example, Fig. 4(c) would look exactly the same whether the 2^{200} vectors were randomly distributed or were organized into 2^{200-m} randomly distributed groups, each consisting of 2^m tightly bunched vectors, provided that the probability to select more than one vector from any group is negligible, i.e., provided that $(4096)^2/2^{200-m} = 2^{m-176} \ll 1$, which is satisfied for $m \lesssim 170$. Indeed, in view of the data in Sec. V A, one expects the vectors to be organized on small angular scales into pairs and quartets and perhaps into somewhat larger groups that persist from the first few steps.

To characterize the angle distribution completely would require the computation of the angles between all pairs among the 2^{200} vectors, which would exhaust the storage and computing power of any computer now and in the foreseeable future. Our results are thus rigorous only up to 12 steps, where we are able to compute the angles between all pairs of vectors. Nonetheless, our results provide some support for the conjecture that the distribution in the chaotic case is essentially random for large numbers of steps. In order to give an approximate picture of such a random distribution, we have developed approximations, shown in Fig. 5, for the information and the trade-off entropy for 2^{200} random vectors in a 512-dimensional Hilbert space.

These approximations are based on knowing $N_{D,\max}(\phi)$, the maximum number of disjoint spheres of radius ϕ that D-dimensional Hilbert space can ac-

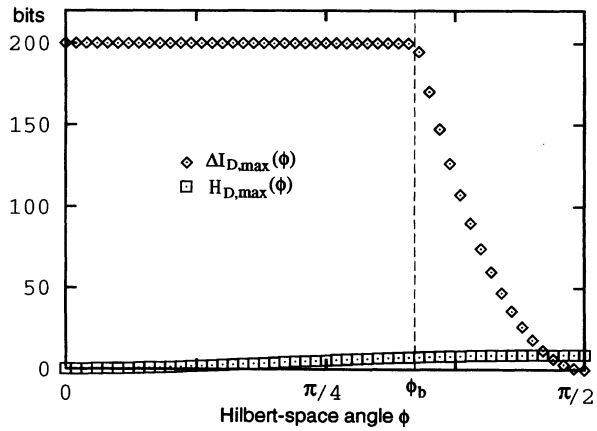

FIG. 5. Upper bounds for the average information $\Delta I_{D,\max}$ and for the trade-off entropy $H_{D,\max}$ for 2^{200} random vectors in 512-dimensional Hilbert space, as given by Eqs. (5.2) and (B10). The curve for $\Delta I_{D,\max}$ is an excellent approximation to the average information $\Delta I(\phi)$, except for a small region around ϕ_b. The trade-off entropy $\Delta H(\phi)$ is well approximated by the curve for $H_{D,\max}(\phi)$ for angles above ϕ_b, but goes to zero rapidly for angles below ϕ_b.

commodate. In Appendix A we compute the volume $\mathcal{V}_D(\phi) = (\sin\phi)^{2(D-1)}\mathcal{V}_D$ contained within a sphere of radius ϕ in D-dimensional Hilbert space [Eq. (A18)] and the total volume $\mathcal{V}_D = \pi^{D-1}/(D-1)!$ of D-dimensional Hilbert space [Eq. (A22)], from which it follows that

$$N_{D,\max}(\phi) = \frac{\mathcal{V}_D}{\mathcal{V}_D(\phi)} = (\sin\phi)^{-2(D-1)} . \tag{5.1}$$

It is worth emphasizing just how enormous Hilbert space is by noting that the number of spheres of radius $\phi = 0.1\,\mathrm{rad}$ that can be accommodated within a D-dimensional Hilbert space is $N_{D,\max} \simeq \phi^{-2(D-1)} = 10^{2(D-1)}$; for the 512-dimensional Hilbert space considered in this paper, this is 10^{1022} spheres.

Suppose N vectors, distributed randomly in D-dimensional Hilbert space, are grouped at resolution level ϕ. The number of groups at this resolution $N(\phi)$ cannot be larger than N, the total number of vectors, nor larger than $N_{D,\max}(\phi)$, the maximum number of groups. For the average information, this entails

$$\begin{aligned}\Delta I(\phi) \le \log_2 N(\phi) &\le \Delta I_{D,\max}(\phi) \\ &\equiv \min[\log_2 N_{D,\max}(\phi), \log_2 N] .\end{aligned} \tag{5.2}$$

One expects a large number of random vectors to fill Hilbert space almost uniformly. For angles ϕ for which $N_{D,\max}(\phi) \ll N$, there are close to $N_{D,\max}(\phi)$ groups with roughly equal numbers of vectors in each group; therefore, for those angles ϕ, $\Delta I(\phi) \simeq \log_2 N_{D,\max}(\phi)$. For angles ϕ for which $N_{D,\max}(\phi) \gg N$, there is just one vector in each group, whence $\Delta I(\phi) \simeq \log_2 N$ for those angles. This means that the upper bound $\Delta I_{D,\max}(\phi)$ is an excellent approximation to $\Delta I(\phi)$ everywhere except for a small region near the sharp bend located at the angle ϕ_b determined by $N_{D,\max}(\phi_b) = N$. The upper bound $\Delta I_{D,\max}(\phi)$ is plotted in Fig. 5 for $D = 512$ and $N = 2^{200}$.

The trade-off entropy, on the other hand, cannot be larger than the maximum entropy of a group, i.e.,

$$\Delta H(\phi) \le H_{D,\max}(\phi) \simeq H_D(\phi) , \tag{5.3}$$

where $H_{D,\max}(\phi)$ [Eq. (B10)] is the maximum possible entropy for a density operator constructed from vectors that lie within a sphere of radius ϕ in D-dimensional Hilbert space, and $H_D(\phi)$ [Eq. (B6)] is the entropy of a uniform distribution of vectors within a sphere of radius ϕ. For large-dimensional Hilbert spaces, there is no appreciable difference between $H_{D,\max}(\phi)$ and $H_D(\phi)$. The maximum entropy $H_{D,\max}(\phi)$ is plotted in Fig. 5 for $D = 512$.

For angles ϕ for which $N_{D,\max}(\phi) \ll N$, where the number of vectors per group is large enough—say, larger than D—the distribution of vectors within each group

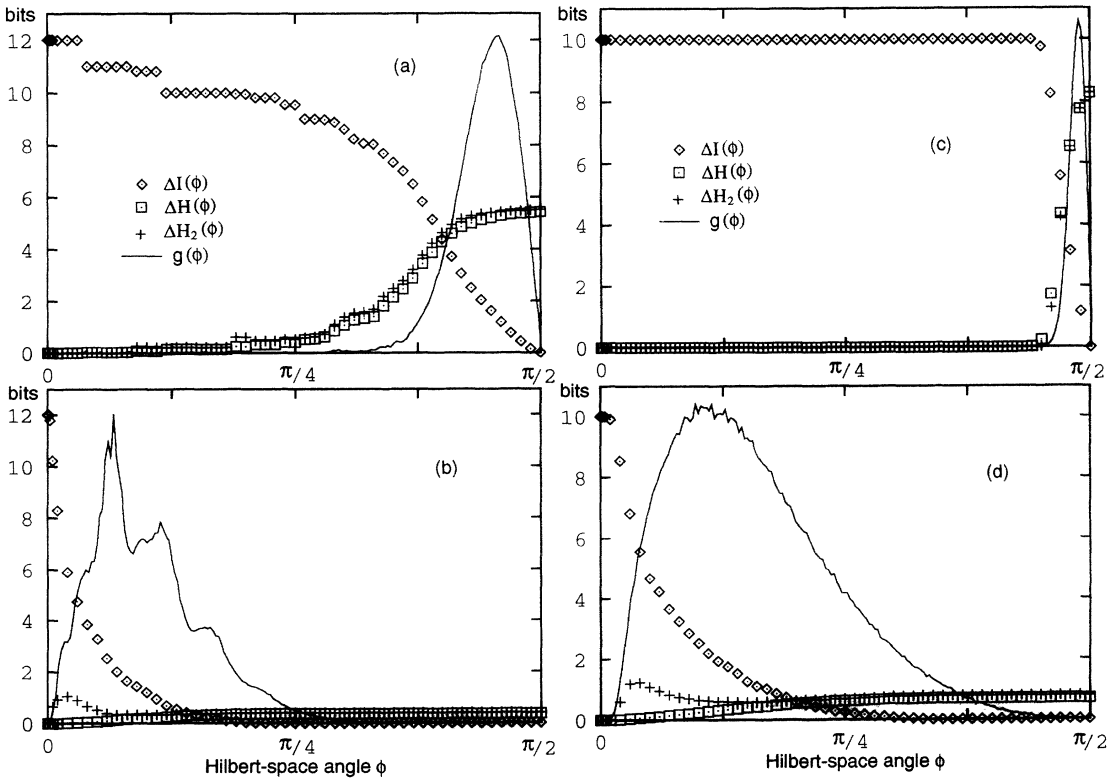

FIG. 6. Same as Fig. 2, but using the turn perturbation (3.2) with $\epsilon = 0.003$. (a) Chaotic case. 12 steps, all 2^{12} vectors. (b) Regular case. 12 steps, all 2^{12} vectors. (c) Chaotic case. 2^{10} vectors randomly chosen after 30 perturbed steps. (d) Regular case. 2^{10} vectors randomly chosen after 30 perturbed steps.

approximates a uniform distribution and thus $\Delta H(\phi)$ is well approximated by $H_D(\phi)$ and hence by $H_{D,\max}(\phi)$. This means that there is a region to the right of ϕ_b in Fig. 5, where $H_{D,\max}(\phi)$ is not only an upper bound, but is also a good approximation to the trade-off entropy. For angles to the left of ϕ_b, the number of vectors in a typical group rapidly approaches 1, which means that the trade-off entropy is very close to zero in the region where the average information saturates.

C. Turn perturbation: $\epsilon = 0.003$

Figure 6 displays results for the turn perturbation, showing the same range of behavior as in the preceding subsections. Figure 6(a) shows how the 2^{12} vectors generated after 12 perturbed steps in the chaotic case fill an $n_d = 46$-dimensional Hilbert space randomly, except for a grouping into pairs, quartets, and perhaps octets, corresponding to the discontinuous drops in $\Delta I(\phi)$. By contrast, in the regular case after 12 steps, displayed in Fig. 6(b), the vectors remain close together and fill just $n_d = 2$ dimensions. Figures 6(c) and 6(d) show 2^{10} vectors chosen randomly out of the 2^{30} vectors generated after 30 perturbed steps. In the chaotic case, the distribution can barely be distinguished from the distribution of random vectors in Fig. 1(a). In the regular case, the vectors are spread a little further apart in comparison with Fig. 6(b), but they still fill only $n_d = 2$ dimensions.

Our results establish well the nearly random character of the distribution of vectors in the chaotic case. This is the main result of this paper, providing numerical evidence for hypersensitivity to perturbations in the quantum kicked top. It is more difficult (and less interesting) to give a general characterization of the distribution of vectors in the regular case. One reason for this is the finite size of the regular region on the classical unit sphere, which makes possible a sort of diffusion of a perturbed vector out of the regular region into the chaotic region. Figure 7 investigates this kind of behavior by showing the distribution of 2^{10} vectors randomly chosen after 100 [Fig. 7(a)] and 200 [Fig. 7(b)] steps in the regular case. It is apparent that the vectors drift more and more apart and begin to explore more dimensions of Hilbert space, although even after 200 steps, the number of explored dimensions is still only $n_d = 5$.

Figure 7(c) shows the eigenvalues of the density operators obtained by averaging over 2^{10} vectors randomly chosen after 30, 100, and 200 perturbed steps in the regular case. The eigenvalues provide a more precise picture of the way additional dimensions are explored, since they are a measure of the relative weight with which the dimensions of Hilbert space are explored. One sees a slow leaking of probability into additional dimensions. This

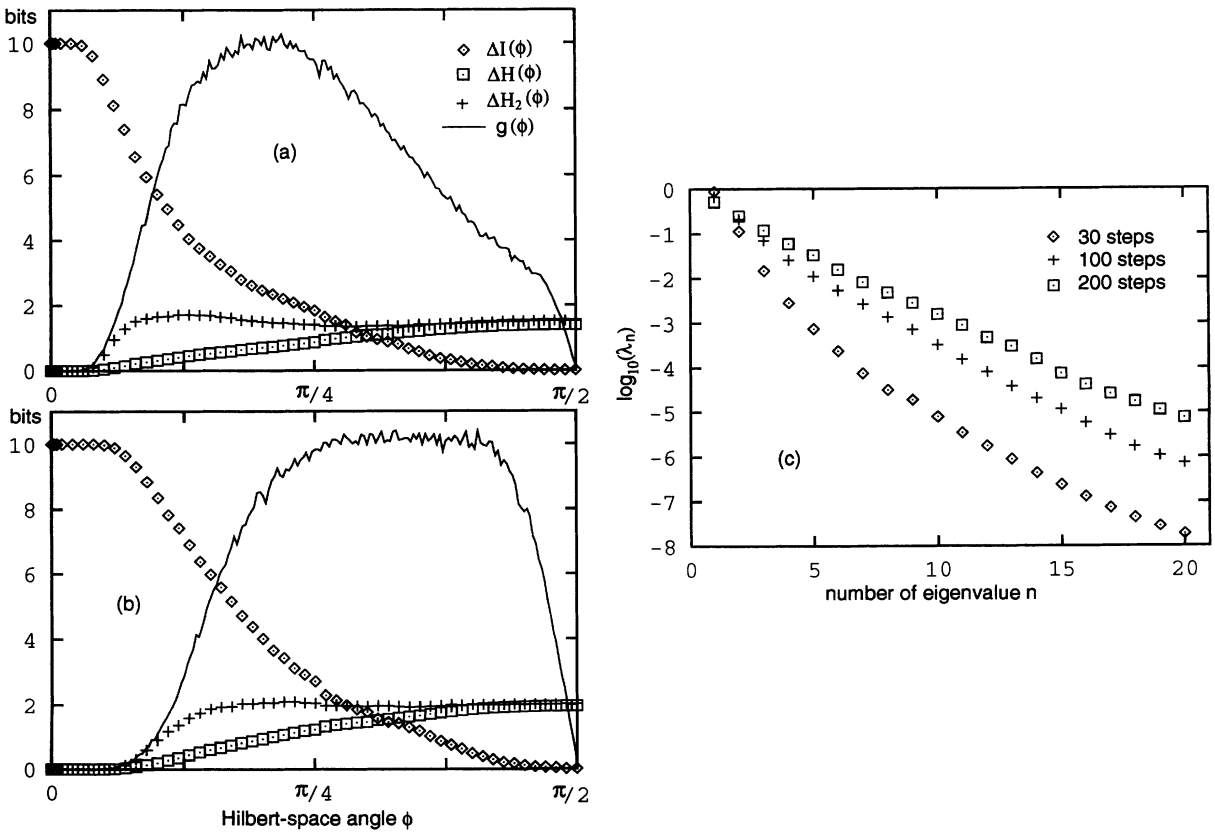

FIG. 7. Same as Fig. 6, regular case. (a) 2^{10} vectors randomly chosen after 100 perturbed steps. (b) 2^{10} vectors randomly chosen after 200 perturbed steps. (c) The 20 largest eigenvalues of the density operators obtained by averaging over 2^{10} vectors randomly chosen after 30, 100, and 200 perturbed steps.

leaking is due to the fact that, with an increasing number of perturbed steps, the probability increases for a state to have significant support outside the regular region, i.e., in the chaotic region. The part of the wave function that is in the chaotic region is subject to chaotic time evolution and therefore free to explore almost all dimensions of Hilbert space.

VI. CONNECTION WITH STATISTICAL PHYSICS

Consider a physical system, classical or quantum, with a known Hamiltonian. The *state* of the system at time $t = t_0$ represents the observer's knowledge of the way the system was prepared. In classical physics, states are described mathematically by a probability density $\rho(\mathbf{x})$ in phase space, while in quantum mechanics, states can be represented either by a Hilbert-space vector $|\psi\rangle$ or, more generally, by a density operator $\hat{\rho}$, depending on the preparation procedure. Observers with different knowledge assign different states to the system; the state is therefore not a property of the system alone, but reflects the observer's state of knowledge about the system.

The entropy (in bits) of a system state, defined in the classical case as $H = -\int d\Gamma \rho(\mathbf{x}) \log_2[\rho(\mathbf{x})]$, where $d\Gamma$ is the usual phase-space measure, and in the quantum case as $H = -\mathrm{Tr}[\hat{\rho}\log_2(\hat{\rho})]$, measures the information missing toward a complete specification of the system. The classical entropy is defined up to an arbitrary additive constant, reflecting the fact that an infinite amount of information would be needed to give the exact location of a single point in phase space. The quantum entropy vanishes for a pure state $\hat{\rho} = |\psi\rangle\langle\psi|$, which is meaningful because no information beyond that contained in the wave function exists about a quantum system. As a consequence of Liouville's theorem, both classical and quantum entropy remain constant under Hamiltonian time evolution.

To make the connection with thermodynamics, we assume that there is a heat reservoir at temperature T_0, to which all energy in the form of heat must eventually be transferred, possibly using intermediate steps such as storage at some lower temperature. In the presence of this fiducial heat reservoir, the free energy or maximum average extractable work for an equilibrium state is given by $F_0 = E - T_0 k_B \ln 2\, H$, where E is the mean internal energy of the state. (More precisely, it is the difference between the F_0 values of two states that determines how much work can be extracted in a transformation between the two states.) It is the main premise of this section that the maximum average extractable work, from now on called *available work*, is given by $F_0 = E - T_0 k_B \ln 2\, H$ *for any state*, even outside equilibrium. This means that each bit of missing information costs one $T_0 k_B \ln 2$ of available work. General arguments for this premise will be given elsewhere [18]; here we discuss just one important case. If the nonequilibrium state was formed through reversible Hamiltonian time evolution starting from an initial equilibrium state, the amount of work $F_0 = E - T_0 k_B \ln 2\, H$ can *in principle* be extracted on average if the system is made to evolve back into the initial equilibrium state using time reversal. This argument is equivalent to Loschmidt's famous *Umkehreinwand* [22]. Although time reversal appears to be impractical in most situations—a remarkable exception is spin echo—there are no known fundamental reasons for excluding it.

Since entropy is a measure of the state of knowledge about the system, and since available work is determined by the entropy, the only way the available work can change (except for changes in the energy levels) is via a change in the state of knowledge. Hamiltonian time evolution of an isolated system does not lead to a change in the state of knowledge; entropy and available work remain unchanged. This is a consequence of Liouville's theorem and is true for regular as well as for chaotic systems: Hamiltonian time evolution in isolated chaotic systems does not lead to information loss [1,2,4]. The following paragraphs discuss the three ways in which information about the system can change: measurement, deliberate discarding of information, and interaction with an incompletely known environment.

Available work can *increase* if an observation is made on the system. The accompanying decrease in entropy does not constitute a violation of the second law of thermodynamics, however, because the physical state of the observer changes in the course of the observation. Landauer [23], following seminal work by Szilard [24], has provided a simple and elegant quantitative description of the change in the state of the observer. If the observer wants to use additional information about the system to increase the available work, he must keep a physical record of the information. According to Landauer's principle, the erasure of a bit of information in the presence of a reservoir at temperature T_0 is necessarily accompanied by dissipation of at least an amount $T_0 k_B \ln 2$ of energy. If this thermodynamic cost of erasing information is taken into account as a negative contribution to free energy, no observation can increase the total available work on the average [25–27]. Information that the observer possesses about the system therefore plays a role complementary to the entropy or missing information. Entropy or missing information about the system reduces the available work through the usual entropy term in the free energy; information the observer actually possesses must be stored physically, thus reducing further the available work due to the Landauer erasure cost. *Total* available work is determined by the sum of entropy and information [25–27,2].

Available work can *decrease* if information about the system is lost. Information loss is equivalent to entropy increase. There are two main mechanisms leading to information loss: deliberate discarding of information and loss of information through interaction with an incompletely known environment. It must be emphasized that the well-known sensitivity to initial conditions in classical chaotic systems does not entail information loss because statistical physics is concerned with the time evolution of probability distributions governed by Liouville's equation, not with trajectories of single phase-space points.

Deliberate discarding of information was used by Jaynes [28–30] to derive traditional thermodynamics.

Jaynes showed how equilibrium thermodynamics follows effortlessly from Liouville's equation if only information about the values of the macroscopic variables defining a thermodynamic state is retained. In Jaynes's approach, irrelevant information is discarded by means of the principle of maximum entropy. Another way to discard information considered irrelevant is coarse graining, where all details of a state below a certain scale are ignored.

In contrast to these examples where information is discarded deliberately, an actual loss of information can occur in a system that, rather than being perfectly isolated, interacts with an incompletely known environment. The interaction with the environment leads to a perturbed time evolution of the system. Predictions for the system state are made by tracing out the environment, i.e., by averaging over the perturbations, which is generally accompanied by an entropy increase.

Nothing forces one, however, to average over the perturbations. Alternatively one could, by making observations on the environment, gather enough information about the perturbations to keep track of the perturbed evolved system state to a certain accuracy, thereby reducing the entropy increase. In Sec. IV, with the accuracy determined by the resolution angle ϕ, the minimum information needed to keep track of the system state to accuracy ϕ was denoted by $\Delta I(\phi)$ and the resulting average entropy increase, the trade-off entropy, was denoted by $\Delta H(\phi)$. Averaging over the perturbations corresponds to an accuracy $\phi = \pi/2$: $\Delta I(\pi/2)$ vanishes and $\Delta H(\pi/2)$ is the entropy due to averaging over the perturbation. Equation (4.12) shows that the sum of information and trade-off entropy is never less than the entropy due to averaging, so that one can never gain in terms of total available work by gathering information about the perturbations. But at this stage, one has no reason to expect that one would do much worse by keeping track of the system state, so that in principle, the system entropy could be kept from increasing.

For a system showing hypersensitivity to perturbation, however, there is a compelling reason not to keep track of a perturbed system state, but to average over the perturbations. The information needed to keep track of a perturbed state increases far more rapidly than the entropy due to averaging, which means that keeping track of the perturbed state would lead to an enormous reduction in available work due to the thermodynamic erasure cost. We have conjectured [1,2,4] that hypersensitivity to perturbation provides a quantitative link between chaos and entropy increase in both classical and quantum open systems. Within the limits of our numerical method, the present paper establishes this link for the quantum kicked top.

ACKNOWLEDGMENT

One of us (R.S.) acknowledges support from the Deutsche Forschungsgemeinschaft.

APPENDIX A: VOLUME CONTAINED WITHIN A SPHERE IN HILBERT SPACE

In this appendix we compute the volume contained within a sphere of radius Φ in D-dimensional Hilbert space. More precisely, we work in projective Hilbert space, i.e., the space of Hilbert-space rays or the space of normalized state vectors in which vectors that differ by a phase factor are equivalent.

We begin by deriving the line element of the Riemannian metric that corresponds to the Hilbert-space angle (2.12). Consider two neighboring normalized state vectors $|\psi\rangle$ and $|\psi\rangle + |d\psi\rangle$. The infinitesimal angle ds between these vectors satisfies

$$1 - ds^2 = \cos^2 ds = |\langle\psi|(|\psi\rangle + |d\psi\rangle)|^2 = 1 + 2\mathrm{Re}(\langle\psi|d\psi\rangle) + |\langle\psi|d\psi\rangle|^2 . \quad \text{(A1)}$$

The normalization of $|\psi\rangle$ and $|\psi\rangle + |d\psi\rangle$ implies that

$$2\mathrm{Re}(\langle\psi|d\psi\rangle) = -\langle d\psi|d\psi\rangle , \quad \text{(A2)}$$

so the line element becomes

$$ds^2 = \langle d\psi|d\psi\rangle - |\langle\psi|d\psi\rangle|^2 = \langle d\psi_\perp|d\psi_\perp\rangle , \quad \text{(A3)}$$

where $|d\psi_\perp\rangle = |d\psi\rangle - |\psi\rangle\langle\psi|d\psi\rangle$ is the projection of $|d\psi\rangle$ orthogonal to $|\psi\rangle$. The metric (A3), called the Fubini-Study metric [31], is the natural metric on projective Hilbert space. Notice that the line element is invariant under phase changes of $|\psi\rangle$ and $|\psi\rangle + |d\psi\rangle$.

Consider now a sphere of radius $\Phi \leq \pi/2$ in projective Hilbert space; let the center of the sphere be denoted by $|\psi_0\rangle$. Any normalized vector $|\psi\rangle$ can be written as

$$|\psi\rangle = e^{i\delta}\cos\phi|\psi_0\rangle + \sin\phi|\eta\rangle , \quad \text{(A4)}$$

where $|\eta\rangle$ is a normalized vector in the subspace orthogonal to $|\psi_0\rangle$ and the polar angle $\phi = \cos^{-1}(|\langle\psi|\psi_0\rangle|)$ satisfies $0 \leq \phi \leq \pi/2$. The region contained within our sphere of radius Φ, which we denote by $V_D(\Phi)$, consists of all vectors such that $\phi \leq \Phi$. The phase freedom in $|\psi\rangle$ can be removed by choosing the phase $\delta = 0$. That having been done, $|\eta\rangle$ ranges over all normalized vectors in the subspace orthogonal to $|\psi_0\rangle$; in particular, two normalized vectors $|\eta\rangle$, differing only by a phase factor, are *not* equivalent.

We can now write

$$|d\psi\rangle = -\sin\phi\, d\phi|\psi_0\rangle + \cos\phi\, d\phi|\eta\rangle + \sin\phi|d\eta\rangle , \quad \text{(A5)}$$

where $|d\eta\rangle$ is the infinitesimal change in $|\eta\rangle$ (notice that $\langle\psi_0|d\eta\rangle = 0$). Normalization of $|\eta\rangle$ and $|\eta\rangle + |d\eta\rangle$ implies, just as in Eq. (A2), that

$$2\mathrm{Re}(\langle\eta|d\eta\rangle) = -\langle d\eta|d\eta\rangle . \quad \text{(A6)}$$

Retaining only second-order terms in the infinitesimal changes, we can put the line element (A3) in the form

$$ds^2 = d\phi^2 + \sin^2\phi\, d\gamma^2 , \quad \text{(A7)}$$

where

$$d\gamma^2 = \langle d\eta | d\eta \rangle - \sin^2\phi\, |\langle \eta | d\eta \rangle|^2 \tag{A8}$$

defines a Riemannian metric on the the space of normalized vectors in the $(D-1)$-dimensional subspace orthogonal to $|\psi_0\rangle$. This space is a $(2D-3)$-dimensional sphere of unit radius, denoted S_{2D-3}, although the line element $d\gamma^2$ is, as we show below, different from the standard geometry on a $(2D-3)$-dimensional unit sphere. Notice that the Fubini-Study metric (A7) scales all lengths on S_{2D-3} by a factor of $\sin\phi$; this scaling is analogous to the way that polar angle on an ordinary 2-sphere scales the size of circles (1-spheres) of latitude.

Consider now any orthonormal basis $|\eta_j\rangle$, $j = 1,\ldots,D-1$, in the subspace orthogonal to $|\psi_0\rangle$. We can introduce coordinates on S_{2D-3} by expanding $|\eta\rangle$ as

$$|\eta\rangle = \sum_{j=1}^{D-1} (x_j + iy_j)|\eta_j\rangle\ . \tag{A9}$$

Normalization of $|\eta\rangle$ implies the constraint

$$1 = \sum_{j=1}^{D-1} x_j^2 + y_j^2\ , \tag{A10}$$

which defines the $(2D-3)$-dimensional unit sphere. The first term in the metric (A8),

$$\langle d\eta | d\eta \rangle = \sum_{j=1}^{D-1} dx_j^2 + dy_j^2\ , \tag{A11}$$

is the flat Euclidean metric in $2(D-1)$ dimensions; it induces the standard metric on S_{2D-3}. The second term in the metric (A8) modifies the standard geometry on S_{2D-3}. Noting that

$$\begin{aligned}\langle \eta | d\eta \rangle &= \frac{1}{2}\, d\left(\sum_{j=1}^{D-1} x_j^2 + y_j^2\right) + i\sum_{j=1}^{D-1} x_j dy_j - y_j dx_j \\ &= i\sum_{j=1}^{D-1} x_j dy_j - y_j dx_j\ ,\end{aligned} \tag{A12}$$

we can put the second term in (A8) in the form

$$\sin^2\phi\, |\langle \eta | d\eta \rangle|^2 = \sin^2\phi \left(\sum_{j=1}^{D-1} x_j dy_j - y_j dx_j\right)^2\ . \tag{A13}$$

Perhaps the easiest way to see how the second term affects the geometry on S_{2D-3} is to make a judicious choice of coordinates. Given an arbitrary vector $|\eta\rangle$, we can always choose the orthonormal basis so that $|\eta_1\rangle = |\eta\rangle$, which means that $|\eta\rangle$ is assigned coordinates $x_1 = 1$, $y_1 = 0$, and $x_j = y_j = 0$, $j = 2,\ldots,D-1$. In these special coordinates the metric (A8), evaluated at $|\eta\rangle$, takes the form

$$d\gamma^2 = \cos^2\phi\, dy_1^2 + \sum_{j=2}^{D-1} dx_j^2 + dy_j^2\ , \tag{A14}$$

where we have used the constraint (A10) to write

$$dx_1 = \frac{1}{x_1}\left(-y_1 dy_1 - \sum_{j=2}^{D-1} x_j dx_j + y_j dy_j\right) = 0 \ \text{ at } |\eta\rangle. \tag{A15}$$

In these special coordinates the standard geometry on S_{2D-3} has the same form at $|\eta\rangle$, except that the $\cos\phi$ is replaced by 1. The effect of the second term in the metric (A8) is thus to shorten lengths (relative to the standard geometry) along one direction on S_{2D-3} by a factor $\cos\phi$; the direction of shortened length corresponds, in the special coordinates, to the y_1 direction or, in coordinate-free language, to an infinitesimal change in the phase of $|\eta\rangle$.

In the special coordinates the volume element on S_{2D-3} at $|\eta\rangle$, defined by the line element $d\gamma^2$, is given by

$$\cos\phi\, dy_1 dx_2 \cdots dx_{D-1} dy_2 \cdots dy_{D-1} = \cos\phi\, d\mathcal{S}_{2D-3}\ , \tag{A16}$$

where $d\mathcal{S}_{2D-3}$ is the volume element defined by the standard geometry on S_{2D-3}. Writing the volume element (A16) in terms of $d\mathcal{S}_{2D-3}$ frees it from dependence on the special coordinates. Referring to the Fubini-Study metric (A7), we can now write the volume element on projective Hilbert space as

$$d\mathcal{V}_D = (\sin\phi)^{2D-3}\cos\phi\, d\phi\, d\mathcal{S}_{2D-3}\ . \tag{A17}$$

The $2D-3$ factors of $\sin\phi$ come from scaling all $2D-3$ dimensions of S_{2D-3}, as required by the Fubini-Study metric (A7).

We are now prepared to compute the volume $\mathcal{V}_D(\Phi)$ contained within a Hilbert-space sphere of radius Φ:

$$\begin{aligned}\mathcal{V}_D(\Phi) &= \int_{V_D(\Phi)} d\mathcal{V}_D \\ &= \int_0^\Phi d\phi\,(\sin\phi)^{2D-3}\cos\phi \int d\mathcal{S}_{2D-3} \\ &= \frac{\mathcal{S}_{2D-3}}{2(D-1)}(\sin\Phi)^{2(D-1)} \\ &= (\sin\Phi)^{2(D-1)}\mathcal{V}_D\ .\end{aligned} \tag{A18}$$

Here $\mathcal{S}_{2D-3}$ is the volume of the unit sphere S_{2D-3}, calculated using the standard geometry (be careful: this is the "area" of S_{2D-3}, not the volume interior to it), and

$$\mathcal{V}_D = \mathcal{V}_D(\pi/2) = \frac{\mathcal{S}_{2D-3}}{2(D-1)} \tag{A19}$$

is the total volume of projective Hilbert space.

The volume of an n-dimensional unit sphere S_n,

$$\mathcal{S}_n = \frac{2\pi^{(n+1)/2}}{\Gamma\left(\dfrac{n+1}{2}\right)}\ , \tag{A20}$$

follows from a standard trick involving Gaussian integrals:

$$\tfrac{1}{2}S_n\,\Gamma\left(\frac{n+1}{2}\right) = \tfrac{1}{2}S_n\int_0^\infty dv\, v^{(n-1)/2}e^{-v}$$
$$= \int_0^\infty dr\, r^n S_n e^{-r^2}$$
$$= \left(\int_{-\infty}^{\infty} du\, e^{-u^2}\right)^{n+1} = \pi^{(n+1)/2}\,. \tag{A21}$$

This gives us $\mathcal{S}_{2D-3} = 2\pi^{D-1}/(D-2)!$, which allows us to write the total volume of projective Hilbert space [31] as

$$\mathcal{V}_D = \frac{\pi^{D-1}}{(D-1)!}\,. \tag{A22}$$

We can obtain immediately two other results: (i) the volume contained between two Hilbert-space spheres of radius ϕ and $\phi + d\phi$ is

$$d\mathcal{V}_D(\phi) = \mathcal{S}_{2D-3}(\sin\phi)^{2D-3}\cos\phi\, d\phi$$
$$= \mathcal{V}_D 2(D-1)(\sin\phi)^{2D-3}\cos\phi\, d\phi\,; \tag{A23}$$

(ii) the probability that two vectors selected at random are separated by a Hilbert-space angle between ϕ and $\phi + d\phi$ is

$$g(\phi)d\phi = \frac{d\mathcal{V}_D(\phi)}{\mathcal{V}_D} = 2(D-1)(\sin\phi)^{2D-3}\cos\phi\, d\phi\,. \tag{A24}$$

APPENDIX B: ENTROPIES OF DISTRIBUTIONS OF VECTORS WITHIN A HILBERT-SPACE SPHERE

In this appendix we compute entropies of density operators constructed from vectors that lie within a sphere of radius Φ in D-dimensional Hilbert space. We first compute the entropy $H_D(\Phi)$ of a density operator $\hat{\rho}$ that corresponds to a uniform distribution of Hilbert-space vectors in the region $V_D(\Phi)$ contained within a sphere of radius Φ. Formally, $\hat{\rho}$ is given by

$$\hat{\rho} = \int_{V_D(\Phi)} \frac{d\mathcal{V}_D}{\mathcal{V}_D(\Phi)}\,|\psi\rangle\langle\psi|\,, \tag{B1}$$

where $\mathcal{V}_D(\Phi) = (\sin\Phi)^{2(D-1)}\mathcal{V}_D$ [Eq. (A18)] is the volume contained within a sphere of radius Φ in D-dimensional Hilbert space, and $d\mathcal{V}_D = (\sin\phi)^{2D-3}\cos\phi\, d\phi\, d\mathcal{S}_{2D-3}$ [Eq. (A17)] is the volume element on projective Hilbert space. Let the center of the sphere be denoted by $|\psi_0\rangle$. Symmetry about $|\psi_0\rangle$ entails that $\hat{\rho}$ have the form

$$\hat{\rho} = \lambda_0\,|\psi_0\rangle\langle\psi_0| + \frac{1-\lambda_0}{D-1}\,(\hat{1} - |\psi_0\rangle\langle\psi_0|)\,. \tag{B2}$$

The eigenvalues of $\hat{\rho}$ are

$$\lambda_0 = \langle\psi_0|\hat{\rho}|\psi_0\rangle = \int_{V_D(\Phi)}\frac{d\mathcal{V}_D}{\mathcal{V}_D(\Phi)}\,|\langle\psi_0|\psi\rangle|^2 = \int_{V_D(\Phi)}\frac{d\mathcal{V}_D}{\mathcal{V}_D(\Phi)}\,\cos^2\phi$$
$$= \frac{\mathcal{S}_{2D-3}}{(\sin\Phi)^{2(D-1)}\mathcal{V}_D}\int_0^\Phi d\phi\,(\sin\phi)^{2D-3}\cos^3\phi = 1 - \frac{D-1}{D}\sin^2\Phi \geq \frac{1}{D} \tag{B3}$$

and

$$\lambda_k = \frac{1-\lambda_0}{D-1} = \frac{\sin^2\Phi}{D} \leq \frac{1}{D}\,,\quad k = 1,\ldots,D-1\,. \tag{B4}$$

The entropy of $\hat{\rho}$ is thus

$$H_D(\Phi) = -\sum_{k=0}^{D-1}\lambda_k\log_2\lambda_k$$
$$= -\lambda_0\log_2\lambda_0 - (1-\lambda_0)\log_2(1-\lambda_0) + (1-\lambda_0)\log_2(D-1) \tag{B5}$$
$$= \left(\frac{D-1}{D}\sin^2\Phi - 1\right)\log_2\left(1 - \frac{D-1}{D}\sin^2\Phi\right) - \frac{D-1}{D}\sin^2\Phi\,\log_2\left(\frac{\sin^2\Phi}{D}\right)\,. \tag{B6}$$

For comparison, the spread of $\hat{\rho}$ [Eq. (4.7)] has its maximum value, regardless of the value of Φ,

$$H_{2,D}(\Phi) = -\sum_{k=1}^{D-1}\frac{\lambda_k}{1-\lambda_0}\log_2\left(\frac{\lambda_k}{1-\lambda_0}\right) = \log_2(D-1)\,, \tag{B7}$$

reflecting the fact that the uniform distribution of vectors within a sphere of radius Φ explores all $D-1$ dimensions in the subspace orthogonal to $|\psi_0\rangle$. This result regarding the spread does not depend on the particular value of λ_0: any density operator of the symmetric form (B2) has the maximum spread $\log_2(D-1)$, provided only that λ_0 is the largest eigenvalue, i.e., $\lambda_0 \geq 1/D$ [cf. Eqs. (4.9) and (B5)].

It is interesting to compare the entropy of a uniform distribution of vectors in $V_D(\Phi)$ with the maximum entropy that can be attained by distributing vectors in $V_D(\Phi)$. To do this, consider a density operator

$$\hat{\rho} = \sum_{i=1}^{N} p_i |\psi_i\rangle\langle\psi_i| \,, \tag{B8}$$

constructed from vectors $|\psi_i\rangle$ that lie in $V_D(\Phi)$, i.e., $|\langle\psi_0|\psi_i\rangle| = \cos\phi_i \geq \cos\Phi$, $i = 1, \ldots, N$.

A unitary transformation in the subspace orthogonal to $|\psi_0\rangle$ leaves the angles ϕ_i and the entropy unchanged. Mixing the density operators that result from all such unitary transformations gives a new density operator which is symmetric about $|\psi_0\rangle$, but which, because of the concavity of the entropy [19,20], has an entropy that is not smaller than the entropy of $\hat{\rho}$. Thus, in seeking the maximum entropy, we can restrict attention to density operators that are symmetric about $|\psi_0\rangle$ and hence have the form (B2) and have entropy given by Eq. (B5). This entropy, which is a function of the eigenvalue λ_0, has a maximum value of $\log_2 D$ at $\lambda_0 = 1/D$ and decreases monotonically away from this maximum in either direction.

The eigenvalue λ_0 is bounded below by

$$\lambda_0 = \langle\psi_0|\hat{\rho}|\psi_0\rangle = \sum_{i=1}^{N} p_i \cos^2\phi_i \geq \cos^2\Phi \,. \tag{B9}$$

Hence an upper bound on the entropy follows from choosing $\lambda_0 = \cos^2\Phi$ when $\cos^2\Phi \geq 1/D$ and choosing $\lambda_0 = 1/D$ when $\cos^2\Phi \leq 1/D$. The upper bound is given by

$$H_{D,\max}(\Phi) = \begin{cases} -\cos^2\Phi \log_2 \cos^2\Phi - \sin^2\Phi \log_2 \sin^2\Phi + \sin^2\Phi \log_2(D-1) \,, & \cos^2\Phi \geq 1/D, \\ \log_2 D, & \cos^2\Phi \leq 1/D \,. \end{cases} \tag{B10}$$

This function is plotted in Fig. 5 for $D = 512$. Notice that the entropy (B6) of a uniform distribution of vectors within a sphere of radius Φ approaches the upper bound (B10) as $D \to \infty$.

That the bound is actually the maximum, as implied by the notation, is demonstrated by finding a density operator, constructed from vectors in $V_D(\Phi)$, which achieves the entropy upper bound. To that end, consider the $2(D-1)$ vectors

$$\begin{aligned} |\psi_j\rangle &= \cos\Phi|\psi_0\rangle + \sin\Phi|\eta_j\rangle \quad j = 1, \ldots, D-1 \\ |\psi'_j\rangle &= \cos\Phi|\psi_0\rangle - \sin\Phi|\eta_j\rangle \,, \quad j = 1, \ldots, D-1 \,, \end{aligned} \tag{B11}$$

where the vectors $|\eta_j\rangle$ make up an orthonormal basis in the subspace orthogonal to $|\psi_0\rangle$. The vectors (B11) all lie on the sphere of radius Φ—as far from $|\psi_0\rangle$ as is allowed. Construct the density operator

$$\begin{aligned} \hat{\rho} &= p_0|\psi_0\rangle\langle\psi_0| + \frac{1-p_0}{2(D-1)} \sum_{j=1}^{D-1} |\psi_j\rangle\langle\psi_j| + |\psi'_j\rangle\langle\psi'_j| \\ &= (\cos^2\Phi + p_0 \sin^2\Phi)|\psi_0\rangle\langle\psi_0| \\ &\quad + \frac{1-p_0}{(D-1)} \sin^2\Phi \,(\hat{1} - |\psi_0\rangle\langle\psi_0|) \,, \end{aligned} \tag{B12}$$

which has the symmetric form of Eq. (B2), with $\lambda_0 = \cos^2\Phi + p_0 \sin^2\Phi$. One would obtain the density operator (B12) by letting $\hat{\rho} - p_0|\psi_0\rangle\langle\psi_0|$ be constructed from any set of vectors that lie on the sphere of radius Φ and are symmetrically distributed about $|\psi_0\rangle$. To achieve the upper bound (B10), one chooses $p_0 = 0$ when $\cos^2\Phi \geq 1/D$ and chooses $p_0 = (1/D - \cos^2\Phi)/\sin^2\Phi$ when $\cos^2\Phi \leq 1/D$.

[1] R. Schack and C. M. Caves, Phys. Rev. Lett. **71**, 525 (1993).

[2] C. M. Caves, in *Physical Origins of Time Asymmetry*, edited by J. J. Halliwell, J. Pérez-Mercader, and W. H. Zurek (Cambridge University, Cambridge, England, 1993), p. 47.

[3] C. M. Caves, Phys. Rev. E **47**, 4010 (1993).

[4] R. Schack and C. M. Caves, Phys. Rev. Lett. **69**, 3413 (1992).

[5] N. L. Balazs and A. Voros, Ann. Phys. (N.Y.) **190**, 1 (1989).

[6] H. Frahm and H. J. Mikeska, Z. Phys. B **60**, 117 (1985).

[7] F. Haake, M. Kuś, and R. Scharf, Z. Phys. B **65**, 381 (1987).

[8] A. Peres, in *Quantum Chaos*, edited by H. A. Cerdeira, R. Ramaswamy, M. C. Gutzwiller, and G. Casati (World Scientific, Singapore, 1991), p. 73.

[9] G. M. D'Ariano, L. R. Evangelista, and M. Saraceno, Phys. Rev. A **45**, 3646 (1992).

[10] J. M. Radcliffe, J. Phys. A **4**, 313 (1971).

[11] P. W. Atkins and J. C. Dobson, Proc. R. Soc. London Ser. A **321**, 321 (1971).

[12] A. M. Perelomov, *Generalized Coherent States* (Springer, Berlin, 1986).

[13] W. K. Wootters, Phys. Rev. D **23**, 357 (1981).

[14] A. M. Perelomov, Commun. Math. Phys. **26**, 222 (1972).

[15] G. J. Chaitin, *Algorithmic Information Theory* (Cambridge University, Cambridge, England, 1987).

[16] R. G. Gallager, *Information Theory and Reliable Communication* (Wiley, New York, 1968).

[17] D. A. Huffman, Proc. IRE **40**, 1098 (1952).

[18] R. Schack and C. M. Caves (unpublished).

[19] R. Balian, *From Microphysics to Macrophysics* (Springer, Berlin, 1991), Vol. 1.
[20] C. M. Caves and P. D. Drummond, Rev. Mod. Phys. **66**, 481 (1994).
[21] W. K. Wootters, Found. Phys. **20**, 1365 (1990).
[22] R. C. Tolman, *The Principles of Statistical Mechanics* (Oxford University Press, Oxford, 1938).
[23] R. Landauer, IBM J. Res. Devel. **5**, 183 (1961).
[24] L. Szilard, Z. Phys. **53**, 840 (1929).
[25] W. H. Zurek, Nature **341**, 119 (1989).
[26] W. H. Zurek, Phys. Rev. A **40**, 4731 (1989).
[27] C. M. Caves, in *Complexity, Entropy, and the Physics of Information*, edited by W. H. Zurek (Addison-Wesley, Redwood City, CA, 1990), p. 91.
[28] E. T. Jaynes, Phys. Rev. **108**, 171 (1957).
[29] E. T. Jaynes, Phys. Rev. **106**, 620 (1957).
[30] E. T. Jaynes, in *Papers on Probability, Statistics, and Statistical Physics*, edited by R. D. Rosenkrantz (Kluwer, Dordrecht, 1983).
[31] G. W. Gibbons, J. Geom. Phys. **8**, 147 (1992).